Optical homogeneous linewidths in glasses in the framework of the soft-potential model

A. J. García and J. Fernández
Departamento de Física Aplicada I, Escuela Técnica Superior de Ingenieros Industriales y de Telecomunicación, Universidad del País Vasco, Alameda de Urquijo s/n, 48013 Bilbao, Spain
(Received 30 December 1996; revised manuscript received 3 March 1997)

The temperature dependence of the optical linewidth of an impurity embedded in a glass matrix is investigated. A model Hamiltonian that couples the impurity to the soft modes characteristic of glasses in the phonon field of the matrix is introduced. We find an excellent agreement between our model predictions and experimental data. We are also able to reproduce supralinear behaviors in the low-temperature regime without any adjustable parameter for the density of states. Finally, the quadratic behavior extending to very low temperatures is explained in terms of the Bose peak equivalent temperature. [S0163-1829(97)04326-9]

I. INTRODUCTION

It has been known for some time that amorphous solids exhibit anomalous behavior when compared with their crystalline counterparts.[1,2] These anomalies include low-temperature specific heat, thermal conductivity, ultrasound propagation, dielectric losses, and optical dephasing, among others. Their most surprising characteristic is universality, i.e., the order of magnitude depends very weakly on the chemical composition of the solid.

An important progress towards the understanding of these anomalies was the introduction by Anderson, Halperin, and Varma,[3] and independently by Phillips,[4] of the so-called tunneling states model (TS model). According to this model, in amorphous solids, together with very long-wavelength acoustic phonons, there is a distribution of low-energy excitations with a two-level system (TLS) structure, which are characterized by quantum-mechanical tunneling through a potential barrier. The TS model provides an explanation for the main characteristics of ultra-low-temperature properties of amorphous solids. Nevertheless, above 1 K, the behavior of these properties deviates from the TS model predictions. Thermal conductivity shows a *plateau* around 10 K, which cannot be explained on the basis of the TS model.[5] Furthermore, in Raman scattering, there appears a peak, known as the Bose peak,[6] which seems to indicate the existence of another kind of low-frequency mode. Neutron spectroscopy measurements have shown these modes to be soft harmonic oscillators with a crossover to anharmonicity at the end of the low-frequency region.[7]

Among the various models proposed to explain these anomalous behaviors above 1 K, it is worth pointing out the soft-potential model (SPM),[8] which gives a unified description of TLS and harmonic modes in terms of soft anharmonic potentials, the so-called soft potentials. This model reproduces the results of the TS model at ultralow temperature, and has allowed one to explain other phenomena at higher temperatures, as is the *plateau* in thermal conductivity[9] and the Raman and neutron data for various materials.[10,11]

The main purpose of our work is to study one of these anomalies of amorphous solids, which, in spite of having been studied in various works, is far from being well explained. We refer to the homogeneous broadening of an impurity transition line embedded in a glass matrix as a function of temperature.[12] The homogeneous linewidth (HLW) of an impurity in these solids shows quantitative and qualitative differences in magnitude and behavior if compared with crystalline solids. In the latter, the HLW follows a T^7 power law for temperatures below the Debye temperature of the glass and a T^2 law above.[13] This behavior can be explained in terms of a two-phonon Raman process in which the impurity levels are coupled to the acoustic phonons of the crystal. However, in amorphous solids, the magnitude of the broadening is some orders of magnitude larger at the same temperature, and follows a T^α power law with α ranging from 1 to 2.6, depending on the material.

Several theoretical models have been proposed to explain such anomalous behaviors.[12] All of them take into account the role of TLS proposed in the TS model. To connect the temperature dependence of the HLW with the TLS a variety of mechanisms has been proposed. They include spectral diffusion of TLS,[14] coupling of the impurity to a TLS that is coupled to the phonon bath,[15–18] coupling to librational modes,[19,20] and use of fractons instead of phonons,[21] to cite some examples. These models predict a variety of behaviors with temperature, depending on the physical mechanism proposed for the dephasing and on the parameters introduced in the model. Nevertheless, none of them can describe the numerous experimental data in a general way.

In this work we calculate the HLW in the framework of the SPM, taking into account the contributions of both kinds of excitations described by this model, namely, TLS and quasiharmonic oscillators (HO), both with a common origin: the soft-potential modes. In Sec. II we introduce the main features of the SPM. In Sec. III we carefully evaluate the density of states predicted by this model, leaving aside some approximations usually accepted in the literature, and we show that numerical evaluation of the density of states has some nontrivial features that reflect on every physical quantity, as the nonlinear exponents ranging between 0.0 and 0.3 usually found experimentally. In Sec. IV we introduce the Hamiltonian model that will be used throughout this work. In Sec. V we present the results obtained for the calculation of the response function of the system in two well-studied regions: the TLS and HO regions, making use of the Zwanzig-Fano theory of irreversibility, which is briefly described in

 © 1997 The American Physical Society

Appendix B. A detailed survey of this calculation is presented in Appendix C. In Sec. VI we evaluate the HLW of the amorphous solid taking the weighed average of the HLW for a specific soft mode, which is the usual approach in the literature, and we find some analytical expressions for this HLW in the TLS and HO regions in some limiting cases. In Sec. VII, numerical evaluations of the exact expressions obtained in Sec. VI are presented. Also, the main features obtained are discussed. In Sec. VIII, some striking points of this model are discussed.

II. THE SOFT-POTENTIAL MODEL

Let us remember the main concepts of SPM.[8] This model proposes the existence of soft localized modes in amorphous solids. The anharmonic potential of one of these modes can be written as

$$V(x)=\mathcal{E}_0[\,\eta(x/a)^2+\xi(x/a)^3+(x/a)^4], \tag{1}$$

where $\mathcal{E}_0$ is an energy of atomic scale, x is the configurational coordinate of the mode, and a is a distance of the order of the interatomic spacing. The values of the dimensionless parameters η and ξ are random due to fluctuations of the structural parameters of the amorphous solid. The soft potentials correspond to $|\eta|,|\xi|\ll 1$. The distribution function of these parameters is given by[22,10]

$$P(\eta,\xi)=|\eta|\mathcal{P}_0(\eta,\xi), \tag{2}$$

where $\mathcal{P}_0(\eta,\xi)$ is even in ξ and slowly varying on both parameters, so it can be taken as a constant in some cases. This point will be discussed in the next section in more detail.

With the aim of introducing the scales of the problem, the following parameter combinations are defined:

$$\eta_L=(\hbar^2/2Ma^2\mathcal{E}_0)^{1/3}, \tag{3}$$

with M the effective mass of the mode, which allows us to introduce the length scale of the system through $a\,\eta_L^{1/2}$, and

$$W=\mathcal{E}_0\,\eta_L^2, \tag{4}$$

which is the characteristic energy of the quartic oscillator, i.e., $\eta=\xi=0$. Also, the abbreviations $\widetilde{\eta}=\eta/\eta_L$ and $\widetilde{\xi}=\xi/\eta_L^{1/2}$ will be used throughout the text.

The interaction of the soft potential (1) with the phonon strain field is given by the bilineal coupling[9]

$$V^{\text{HO-PH}}(x)=\sum_\sigma \Lambda_\sigma x e_\sigma, \tag{5}$$

where e_σ is the phonon strain field in branch σ and Λ_σ the corresponding coupling constant in that branch. The relation between these coupling constants and the deformation potentials, γ_σ, of the TS model is given by[23]

$$\gamma_\sigma=\Lambda_\sigma\sqrt{|\widetilde{\eta}|/2}. \tag{6}$$

In the region $\eta<\frac{9}{32}\xi^2$ the potential (1) has a double-well structure. If $|\widetilde{\xi}||\widetilde{\eta}|<1$ and, at the same time, η is negative and within the limits $|\eta|>3\,\eta_L$, the two lowest levels of the potential (1) form a TLS. The eigenstates, $|+\rangle,|-\rangle$, of this TLS have eigenenergies $+E/2$ and $-E/2$, respectively, with

$$E=\sqrt{\Delta^2+\Delta_0^2} \tag{7}$$

being the energy splitting.[24] Δ_0 is the so-called tunnel splitting parameter, and Δ the asymmetry, which can be expressed in terms of the SPM parameters through

$$\Delta_0\approx W\,\exp\left[-\frac{\sqrt{2}}{3}\,|\widetilde{\eta}|^{3/2}\right], \tag{8}$$

$$\Delta=\frac{W}{\sqrt{2}}\,|\widetilde{\xi}||\widetilde{\eta}|^{3/2}. \tag{9}$$

In the region $\eta>\frac{9}{32}\xi^2$ the potential (1) has a one-well structure. In the limit $1\gg\eta\gg\eta_L$ the excitations in the well are nearly harmonic, with a level spacing given by

$$E=2W\sqrt{|\widetilde{\eta}|}, \tag{10}$$

and their eigenfunctions are those of a harmonic oscillator.

III. THE DENSITY OF STATES OF TLS AND HO

It is important to make some considerations about the distribution function (2) and the density of states of TLS and HO derived from it. One of the main hypothesis of SPM (Ref. 10) consists in taking the function $\mathcal{P}_0(\eta,\xi)$ as a constant, $\mathcal{P}_0(\eta,\xi)\cong\mathcal{P}_0(0,0)\equiv P_0$. Some of the anomalies above 1 K in amorphous solids could been explained with this distribution function, as is the *plateau*[9] in thermal conductivity or the minimum in the function C_p/T^3 (C_p denotes specific heat, T denotes temperature),[10] for example. Nevertheless, some other nontrivial features found experimentally have no easy explanation in the framework of the SPM. This is the case of the second rise of thermal conductivity at the end of the *plateau* and the maximum in C_p/T^3.[25,26] Ramos, Gil, and Buchenau (see Ref. 25) have shown that a small modification of the parameter distribution (2) is able to describe these last two phenomena, explaining in this way the main thermal anomalies in amorphous solids in the whole low-temperature range (see Appendix A). This will be the distribution function from which we shall start. So, the distribution of parameters of the potential (1) is given by

$$P(\eta,\xi)=|\eta|\mathcal{P}_0(\eta,\xi)=P_0|\eta|\exp\left[-\frac{A}{\eta_L^3}\left(\frac{\eta\xi}{2}-\frac{\xi^3}{8}\right)^2\right], \tag{11}$$

where $A=0.169(W/k_BT_g)^{3/2}$, with k_B the Boltzmann constant and T_g the transition temperature of the glass.

In the following, let us consider the densities of states derived from this distribution function.

A. Density of states of TLS

As explained above, in the soft-modes region, $|\eta||\xi|\ll 1$, so the dominant term in the exponent of Eq. (11) is the first one. Moreover, in the TLS region, $|\eta||\xi|<\eta_L^{3/2}$, so $P_0\geqslant P(\eta,\xi)>P_0\,\exp(-A)$. For example, in the case of amorphous SiO_2, $A=2.21\times10^{-5}$ (see Table I). So, in this region, the distribution function (11) goes back to that of the SPM:

$$P(\eta,\xi)=P_0|\eta|. \tag{12}$$

TABLE I. SPM and fitting parameters.

	Substance			
	SiO_2	Silicate	GeO_2	PMMA
Sound wave parameterse				
ρ (kg/m^3)[a]	2200	2400	3600	1200
ν_1 (m/s)[b]	5800	5300[c]	3900[c]	3150
ν_t (m/s)[b]	3800	3200[c]	2340[c]	1570
SPM parameters				
P_s (10^{23} states/m^3)[d]	0.99	3.91	1.17	1.27
W/k_B (K)[d]	3.8	7.20	3.8	2.52[a]
Λ_1 (eV)[b]	0.65	0.37	0.56	0.15
Λ_t (eV)[b]	0.41	0.25	0.35	0.11
Fit parameters				
b (eV Å^3)	6.3×10^{-2}	2.3×10^{-1}	4.8×10^{-1}	3.6
V_c (Å^3)	543	1143	555	4354
$\tilde{\eta}_{\min}$	7.03	14.11	20.90	17.23
Glass temperatures				
E_b/k_B (K)	49.9	67.3	43.2	26.0
T_g (K)[b]	1473	717	830	374
Θ_D (K)[a]	494	436	307	256
N_s (molecules)	12[e]	31	11.5	36

[a]Reference 27.
[b]Reference 28.
[c]Calculated according to Ref. 28.
[d]Reference 25.
[e]Reference 10.

The energy density of states is given by

$$n^{\mathrm{TLS}}(E)=\int_{-\infty}^{0}d\eta\int_{-\infty}^{+\infty}d\xi\ P(\eta,\xi)\,\delta(E-E'(\eta,\xi)). \tag{13}$$

Going to the variables (E,η) we have

$$P(E,\eta)=\frac{\sqrt{2}P_0\eta_L^2}{W}\frac{E}{\sqrt{|\eta|}\sqrt{E^2-\Delta_0^2(\eta)}}, \tag{14}$$

and integrating with the aid of the Dirac delta function, we get

$$n^{\mathrm{TLS}}(E)=\frac{\sqrt{2}}{W}P_s\int_{\tilde{\eta}_0}^{\tilde{\eta}_{\min}}\frac{d\tilde{\eta}}{\sqrt{\tilde{\eta}}}\frac{E}{\sqrt{E^2-\Delta_0^2}}. \tag{15}$$

In this expression $P_s=2P_0\eta_L^{5/2}$, $\tilde{\eta}_0=\tilde{\eta}(\Delta_0=E)$ [see expression (8)] if $E<W$, and $\tilde{\eta}_0=0$ if $E>W$; $\tilde{\eta}_{\min}$ is introduced so that the density of states remains finite, and it is fixed by the duration of the experiment, t_{expt}. In fact, following Ref. 10, the only TLS that make a contribution are those that have undergone a transition during t_{expt}. On the other side, for small values of E/k_BT, we can estimate the characteristic decay time of those TLS with a small asymmetry by[9]

$$\tau^{-1}=\tau_0^{-1}(E)\frac{|\tilde{\eta}|}{2}\left(\frac{\Delta_0}{W}\right)^2, \tag{16}$$

where $\tau_0^{-1}(E)=(W^2E/2\pi\rho\hbar^4)\Sigma_\sigma\Lambda_\sigma^2/\nu_\sigma^5$. Making use of Eqs. (16) and (8) we arrive at the condition that fixes $\tilde{\eta}_{\min}$:

$$\frac{2\tau_0(E)}{t_{\mathrm{expt}}}=\tilde{\eta}_{\min}\exp\left[-\frac{2\sqrt{2}}{3}\tilde{\eta}_{\min}^{3/2}\right]. \tag{17}$$

For example, in the case of amorphous SiO_2, assuming $W/E=10$ and $t_{\mathrm{expt}}=10^2$ s, we obtain $\tau_0\cong9.6\times10^{-9}$ s, $\tilde{\eta}_{\min}\cong8.78$.

A commonly used approximation consists in neglecting the term Δ_0^2 in the square root in expression (15), provided $\tilde{\eta}_{\min}>1/\eta_L$.[10,22] With this simplification we arrive at an expression that does not depend on the energy spacing E and is slightly dependent on t_{expt}

$$n^{\mathrm{TLS}}=2\sqrt{2}\frac{\sqrt{\tilde{\eta}_{\min}}P_s}{W}. \tag{18}$$

Nevertheless, a numerical evaluation of expression (15) leads to densities of states the same as those shown in Fig. 1 for amorphous SiO_2, for different values of t_{expt}, which are only constant for $E\gg W$. In this figure, we also compare the exact density of states (15) with the approximated one (18) for a fixed value of t_{expt}. The temporal dependence of the density of states is also shown. The deviations from the constant value predicted by Eq. (18) reflects on the behavior of physical quantities.

B. Density of states of HO

Following Ref. 25, the density of states of a HO is given by

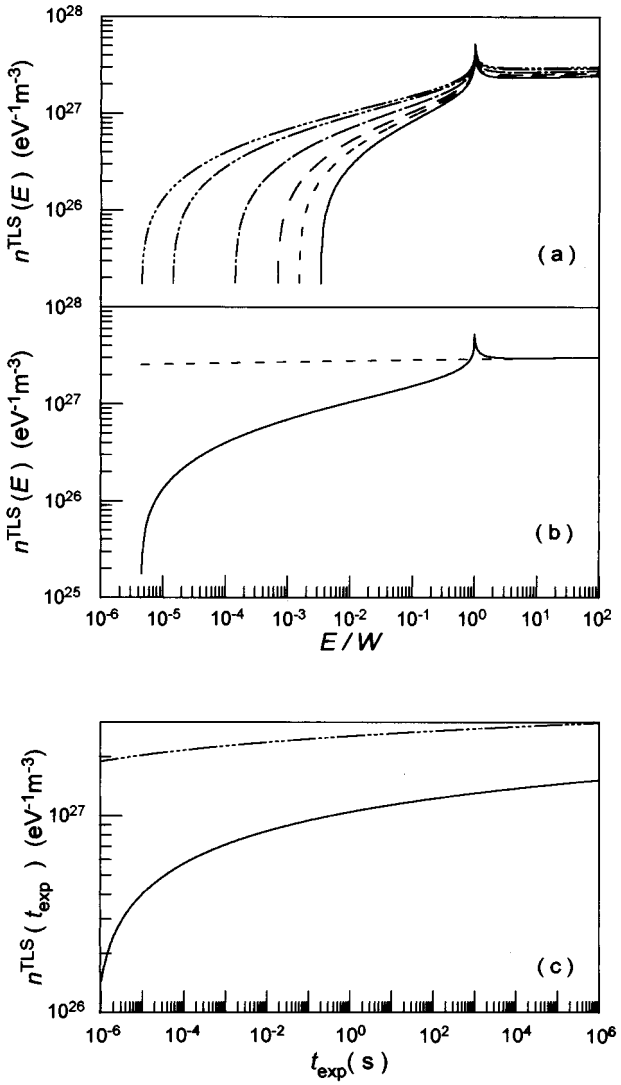

FIG. 1. TLS density of states. (a) Density of states for various experiment durations: (—): $t_{expt}=10^{-2}$ s; (- - -): $t_{expt}=10^{-1}$ s; (– -): $t_{expt}=1$ s; (–·–·): $t_{expt}=10^{2}$ s; (–···–): $t_{expt}=1$ d; (–····–): $t_{expt}=1$ month. (b) Comparison between the density of states (15) and the one given by (18) for $t_{expt}=1$ month. (c) Temporal dependence of the density of states: $E/W=0.1$ (—), $E/W=10$ (–····–).

$$n^{\mathrm{HO}}(E)=\frac{P_s}{6\sqrt{2}W}\left(\frac{E}{W}\right)^4\int_0^1 dz\ \exp[-A(E/2W)^6z^2(1-z^2)^2]. \tag{19}$$

Instead of considering this density of states directly, we shall use two limiting cases that reflect the main features of Eq. (19) and are easier to manage:[29]

$$n^{\mathrm{HO}}(E)=\begin{cases}\dfrac{P_s}{6\sqrt{2}W}\left(\dfrac{E}{W}\right)^4 & \text{for } A\left(\dfrac{E}{W}\right)^6\ll 1\\ \dfrac{P_s}{W}\left(\dfrac{\pi}{2A}\right)^{1/2}\left(\dfrac{E}{W}\right) & \text{for } A\left(\dfrac{E}{W}\right)^6\gg 1.\end{cases} \tag{20}$$

In the first of them we see that the density of states reduces to the one commonly used in the SPM framework.[9] For this simplified density of states, the energy of the maximum in $n^{\mathrm{HO}}(E)/E^2$ is given by

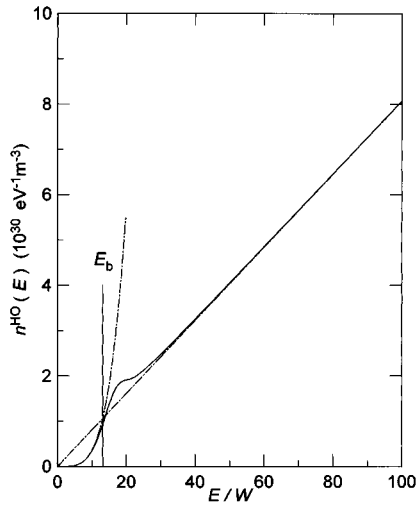

FIG. 2. HO density of states. (—): calculated from Eq. (19); (–·–·): calculated from Eq. (20). Also the value of the Bose peak energy is shown.

$$E_b=2.2W/A^{1/6}, \tag{21}$$

in good agreement with the value obtained directly from Eq. (19) (see Ref. 25). So, our simplified density of states is able to describe the maximum observed in specific heat data and also in the Raman and neutron scattering data, usually referred to as the Bose peak. Following Ref. 25, we shall take E_b as the upper limit of what we call soft modes.

In Fig. 2, the exact density of states (19) and the approximated one (20) are presented. It can be seen that our approximated density of states describes the main features of the HO density of states.

IV. THE HAMILTONIAN MODEL

With the previous considerations, we can introduce our Hamiltonian model to study the HLW of an impurity embedded in an amorphous solid.

Following the usual hypothesis,[15,16] the resonant optical transition takes place between two levels of the impurity ($\alpha=0$ with energy ϵ_0 and $\alpha=1$ with energy ϵ_1), with an energy difference $\hbar\omega_0=\epsilon_1-\epsilon_0$, which we shall suppose to be much greater than the Debye energy of the matrix and the soft-mode maximum energy.

The Hamiltonian of the impurity interacting with a soft mode in the phonon field is given by

$$H=\sum_{\alpha=0}^{1}\epsilon_\alpha a_\alpha^\dagger a_\alpha+H^{\mathrm{SM}}(x)+\sum_q\hbar\omega_q n_q+\sum_{\alpha=0}^{1}g_\alpha a_\alpha^\dagger a_\alpha x+\sum_\sigma\Lambda_\sigma x e_\sigma. \tag{22}$$

In this expression, the fermionic operators $a_\alpha^\dagger$, a_α describe the electronic levels of the impurity, $H^{\mathrm{SM}}(x)$ is the Hamiltonian of the soft mode (see Sec. II), the third term is the Hamiltonian of the phonon field where $q=(\mathbf{q},\sigma)$, whereas the two last terms describe the interaction of the soft mode with the electronic levels of the impurity and the interaction of the soft mode with the phonons, respectively. g_α are the

soft-mode–impurity coupling constants. The soft-mode–impurity interaction has been assumed to be diagonal, which is nothing but the mathematical expression of the hypothesis made in the previous paragraph.

Once the Hamiltonian has been stated, we can study the response of the system to an external electromagnetic perturbation, which will be accomplished in the following sections.

V. LINE-SHAPE CALCULATION FOR THE IMPURITY–SM-PHONONS SYSTEM

Let us consider the system described in Sec. IV and let us study the response function of this system under the action of an external electromagnetic field in the framework of the Zwanzig-Fano relaxation theory (which is briefly described in Appendix B). Let us introduce some new notation that will be used throughout the rest of this section:

We can rewrite Hamiltonian (22) as

$$H=H^{(S)}+H^{(B)}+H_{\rm int}, \tag{23}$$

where $H^{(S)}$ refers to the optically active subsystem (the impurity+soft mode subsystem), $H^{(B)}$ refers to the bath subsystem (the phonon field), and $H_{\rm int}$ refers to the interaction between both subsystems. The interaction between the optically active subsystem (OAS) and the thermal bath can be factorized as

$$H_{\rm int}=V^{(S)}V^{(B)}, \tag{24}$$

where $V^{(S)}$ depends on the OAS variables and $V^{(B)}$ on the bath variables, respectively.

As the potential (1) cannot be analytically solved, we shall study the response of the system in the two limiting regions introduced in Sec. II, the TLS and HO regions.

A. Response function in the TLS region

In the TLS region, the Hamiltonian (22) can be expressed in the TLS basis in terms of the energy splitting, the asymmetry, and the tunnel splitting parameter. The expression obtained in that basis is

$$\begin{aligned}H=&\sum_{\alpha=0}^{1}\epsilon_\alpha a_\alpha^\dagger a_\alpha+\frac{E}{2}\sigma_z+(\Delta\sigma_z+\Delta_0\sigma_x)/E\sum_{\alpha=0}^{1}\tilde g_\alpha a_\alpha^\dagger a_\alpha\\&+\sum_q\hbar\omega_q n_q+i(\Delta\sigma_z+\Delta_0\sigma_x)/E\\&\times\sum_q\sqrt{\hbar\omega_q/2\rho\nu_\sigma^2}\Lambda_\sigma\sqrt{|\tilde\eta|/2}(b_q-b_q^\dagger),\end{aligned} \tag{25}$$

where σ_i is the ith Pauli matrix and $\tilde g_\alpha=g_\alpha\sqrt{|\tilde\eta|/2}$. The bosonic operator b_q ($b_q^\dagger$) stands for the annihilation (creation) of a phonon in the q mode. ρ is the mass density of the amorphous solid and ν_σ is the sound velocity in branch σ. This Hamiltonian is the one by Lyo,[15,16] as we can easily see by identifying

$$\begin{aligned}V_\alpha^z&=-2\tilde g_\alpha\Delta/E,\\V_\alpha^\pm&=-\tilde g_\alpha\Delta_0/E,\end{aligned} \tag{26}$$

where V_α^i are the coupling constants defined by Lyo.

We can also make the following identifications:

$$H^{(S)}=\sum_{\alpha=0}^{1}\epsilon_\alpha a_\alpha^\dagger a_\alpha+\frac{E}{2}\sigma_z+(\Delta\sigma_z+\Delta_0\sigma_x)/E\sum_{\alpha=0}^{1}\tilde g_\alpha a_\alpha^\dagger a_\alpha, \tag{27}$$

$$H^{(B)}=\sum_q\hbar\omega_q n_q, \tag{28}$$

$$V^{(S)}=(\Delta\sigma_z+\Delta_0\sigma_x)/E, \tag{29}$$

$$V^{(B)}=i\sum_q\sqrt{\hbar\omega_q/2\rho\nu_\sigma^2}\Lambda_\sigma\sqrt{|\tilde\eta|/2}(b_q-b_q^\dagger). \tag{30}$$

The OAS Hamiltonian can be diagonalized, and its eigenvalues are given by

$$E_n^\alpha=\epsilon_\alpha+\frac{n}{2}\sqrt{\Delta_0^2+(\Delta-2\tilde g_\alpha)^2}=\epsilon_\alpha+\frac{n}{2}\varepsilon_\alpha, \tag{31}$$

with $n=\pm1$, and its eigenstates

$$\begin{aligned}|\alpha,-1\rangle&=(\sin\phi_\alpha|-\rangle-\cos\phi_\alpha|+\rangle)|\alpha\rangle,\\|\alpha,+1\rangle&=(\cos\phi_\alpha|-\rangle+\sin\phi_\alpha|+\rangle)|\alpha\rangle,\end{aligned} \tag{32}$$

where the first index, α, refers to the impurity state, and the second one to the TLS state and

$$\sin\phi_\alpha=(1/\sqrt2)\sqrt{1-(E-2\tilde g_\alpha\Delta/E)/\varepsilon_\alpha}, \tag{33}$$

$$\cos\phi_\alpha=(1/\sqrt2)\sqrt{1+(E-2\tilde g_\alpha\Delta/E)/\varepsilon_\alpha}. \tag{34}$$

From this new basis we have

$$H^{(S)}=\sum_{\alpha=0}^{1}\sum_{n=-1}^{1}E_n^\alpha|\alpha,n\rangle\langle\alpha,n|, \tag{35}$$

$$V^{(S)}=\sum_{\alpha=0}^{1}(-A_\alpha\sigma_z^\alpha+B_\alpha\sigma_x^\alpha), \tag{36}$$

with

$$\sigma_i^0=\begin{pmatrix}0_{2\times2}&0_{2\times2}\\0_{2\times2}&\sigma_i\end{pmatrix},\quad\sigma_i^1=\begin{pmatrix}\sigma_i&0_{2\times2}\\0_{2\times2}&0_{2\times2}\end{pmatrix}$$

(Ref. 30) and

$$A_\alpha=(\Delta/E)\cos2\phi_\alpha+(\Delta_0/E)\sin2\phi_\alpha, \tag{37}$$

$$B_\alpha=(\Delta/E)\sin2\phi_\alpha-(\Delta_0/E)\cos2\phi_\alpha. \tag{38}$$

Using expressions (30), (35), and (36) we arrive at an expression for the response function of the system in the TLS region given by (see Appendix B)

$$F^{\mathrm{TLS}}(\omega,E) \cong \frac{1}{\pi}|\mu_{10}^{\mathrm{ion}}|^2 \sum_{n=-1}^{1}\sum_{m=-1}^{1} \times \frac{(S_{n,m}^{\mathrm{TLS}})^2 \rho_{0m,0m}^{(S)} \Gamma_{1n,0m}^{\mathrm{TLS}}}{(\hbar\omega-\hbar\omega_0-n\varepsilon_1/2+m\varepsilon_0/2-\delta_{1n,0m}^{\mathrm{TLS}})^2+(\Gamma_{1n,0m}^{\mathrm{TLS}})^2}. \tag{39}$$

In this expression, μ_{10}^{ion} is the impurity dipole moment nondiagonal element, that allows the electronic transition. $\rho_{0m,0m}^{(S)}$ is the OAS density matrix diagonal element with the impurity in its ground state. It is given by

$$\rho_{0m,0m}^{(S)} = \exp(-m\beta\varepsilon_0/2)/2\cosh(\beta\varepsilon_0/2). \tag{40}$$

The elements $S_{n,m}^{\mathrm{TLS}}$ are the overlap integrals of the OAS wave functions between the states with the impurity in its ground state and in its excited state, i.e., $(S_{n,m}^{\mathrm{TLS}})^2=|\langle 1,n|0,m\rangle|^2$. They are given by

$$(S_{n,m}^{\mathrm{TLS}})^2 = \begin{cases} \cos^2(\phi_1-\phi_0), & n=m \\ \sin^2(\phi_1-\phi_0), & n\neq m. \end{cases} \tag{41}$$

The functions $\delta_{1n,0m}^{\mathrm{TLS}}(E)$ and $\Gamma_{1n,0m}^{\mathrm{TLS}}(E)$ are worthy of special attention. As can be seen from expression (39), $\delta_{1n,0m}^{\mathrm{TLS}}(E)$ is the shift of the transition that begins at level $(0,n)$ (the impurity is excited and the TLS reaches level m) and ends at level $(1,m)$. This shift is due to the interaction with the thermal phonon field. $\Gamma_{1n,0m}^{\mathrm{TLS}}(E)$ stands for the half-width of that transition, and is given by the sum of the levels involved in the transition; i.e., due to the interaction with the thermal bath, the OAS levels take a finite lifetime. The expressions for these two magnitudes are (see Appendix C)

$$\delta_{1n,0m}^{\mathrm{TLS}}(E,\Delta_0)=\delta_0^{\mathrm{TLS}}(E)[2n\varepsilon_1B_1^2(k_BT)^2\Xi_1(T)-2m\varepsilon_0B_0^2(k_BT)^2\Xi_0(T)+B_1^2(k_BT)^3\Omega_{1n}(T)-B_0^2(k_BT)^3\Omega_{0m}(T) +(A_0^2-A_1^2)(k_B\Theta_D)^3/3]. \tag{42}$$

$$\Gamma_{1n,0m}^{\mathrm{TLS}}(E,\Delta_0)=\Gamma_0^{\mathrm{TLS}}(\Delta_0)\{B_1^2\varepsilon_1^3[n_B(\varepsilon_1)+(1+n)/2]+B_0^2\varepsilon_0^3[n_B(\varepsilon_0)+(1+m)/2]\}. \tag{43}$$

In both of these expressions, n_B stands for the Bose-Einstein distribution function and Θ_D is the Debye temperature. The following definitions also have been introduced:

$$\delta_0^{\mathrm{TLS}}(\Delta_0)=\sum_\sigma \Lambda_\sigma^2|\tilde{\eta}|/8\pi^2\rho\hbar^3\nu_\sigma^5, \tag{44}$$

$$\Gamma_0^{\mathrm{TLS}}(\Delta_0)=\pi\delta_0^{\mathrm{TLS}}(\Delta_0), \tag{45}$$

$$\Xi_\alpha(T)=\int_0^{\Theta_D/T} dx\, x^3 n_B(x)/[(\beta\varepsilon_\alpha)^2-x^2], \tag{46}$$

$$\Omega_{\alpha n}(T)=\int_0^{\Theta_D/T} dx\, x^3/(n\beta\varepsilon_\alpha-x). \tag{47}$$

Let us briefly mention the approximations that led to expression (39).

Antiresonant terms in $\hbar\omega+\hbar\omega_0$ have been neglected as, in the vicinity of the resonance, they are very small when compared to the resonant one in Eq. (39). The memory function has been evaluated to second order in the phonon strain field; i.e., this calculation is only valid for small values of the strain field. We have made use of the Markovian approximation,[31] which consists in assuming that the thermal bath memory is infinitely short.

Under these approximations, the response function of the system described by Hamiltonian (25) is given by four Lorentzian lines, corresponding to the four possible optical transitions between levels $(0,m)$ and $(1,n)$, each of these lines being centered at an energy $n\varepsilon_1/2-m\varepsilon_0/2+\delta_{1n,0m}^{\mathrm{TLS}}(E,\Delta_0)$ relative to the impurity transition energy. Each of these Lorentzian lines has a half-width given by $\Gamma_{1n,0m}^{\mathrm{TLS}}(E,\Delta_0)$ and its intensity is weighed by a thermal factor, the OAS density matrix elements, and an overlap one, the $S_{n,m}^{\mathrm{TLS}}$ elements.

It is obvious that extracting any information from expression (39) is a difficult task. There is, however, a limiting case where the expression for the line shape is simple. So, in the limit $\Delta_0 \ll \Delta$, the following simplifications can be made:

$$(S_{n,m}^{\mathrm{TLS}})^2 = \begin{cases} 1 & n=m \\ 0 & \text{otherwise}, \end{cases} \tag{48}$$

$$B_\alpha = 0,$$

$$A_\alpha = -1, \tag{49}$$

$$\delta_{1n,0m}^{\mathrm{TLS}}(E)=0, \tag{50}$$

and the response function can be written as

$$F^{\mathrm{TLS}}(\omega)=|\mu_{10}^{\mathrm{ion}}|^2 \sum_{n=-1}^{1} \frac{\rho_{0n,0n}\Gamma_{1n,0n}^{\mathrm{TLS}}}{(\hbar\omega-\hbar\omega_0-nV^z/2)^2+(\Gamma_{1n,0n}^{\mathrm{TLS}})^2}, \tag{51}$$

with $V^z=V_1^z-V_0^z\cong 2\tilde{g}_0-2\tilde{g}_1$.

So, in this limit, the response function is formed by two Lorentzian lines shifted by a quantity $\pm V^z/2$ from the impurity transition energy. Expression (51) coincides with that by Lyo[15,16] in the limit of diagonal-impurity–TLS coupling and slow modulation, i.e., $V^z \gg 4\Gamma_{1n,0-n}^{\mathrm{TLS}}$, being $2\Gamma_{1n,0-n}^{\mathrm{TLS}}/\hbar=\tau^{-1}$ the inverse of the TLS lifetime [compare with expression (16)]. However, our response function (39) only contains the slow modulation part, contrarily to the one by Lyo for diagonal modulation, which is valid for the fast modulation limit also. This is due to the fact that we have considered

the impurity+TLS system as a coherent state, which is meaningful only if the coupling is strong enough to form such a state ($V^z \gg 4\Gamma^{\rm TLS}_{1n,0-n}$), as has been already explained by Lyo.[16]

In addition, if we take the weak coupling limit in expression (51), i.e., $E \gg V^z \gg 4\Gamma^{\rm TLS}_{1n,0-n}$, we shall have

$$\Gamma^{\rm TLS}_{1n,0n} = \Gamma^{\rm TLS}_0 \Delta_0^2 E[2n_B(E)+1+n], \tag{52}$$

$$\rho_{0n,0n} = \exp(-n\beta E/2)/2\,\cosh(\beta E/2). \tag{53}$$

As we shall later see, it is enough to consider this limit in order to explain the experimental data.

All the previous expressions in this section have been calculated for a specific TLS of spacing E. However, in an amorphous solid, there is a set of these TLS (soft modes in general), the parameters of which are distributed according to Eq. (12). So, to obtain the whole response of the amorphous solid, it is necessary to average the response function for a specific excitation with the adequate distribution function.

As pointed out by some authors,[15,18] we can expect the impurity-TLS coupling to vary with the distance in between, so an additional average over these couplings has to be performed. So, the total response function of the amorphous solid will be given by

$$\mathcal{F}^{\rm TLS}(\omega) = 2\pi \int dE\; d\eta\; P(E,\eta) \int_0^{r_c} dr\; F^{\rm TLS}(\omega,E,\eta). \tag{54}$$

The cutoff in the spatial integration is introduced in order to guarantee we are in the slow modulation limit, where expression (39) is valid. As a microscopic description of the soft modes is lacking, it is difficult to give the exact dependence of the coupling with distance. So, we shall follow the usual hypothesis accepted in the literature and assume a dipole-dipole interaction between the impurity and TLS.[15] The cutoff radius is then given by

$$V^z = b/r_c^3 = 4\Gamma^{\rm TLS}_{1n,0-n} = 2\Gamma^{\rm TLS}_0 \Delta_0^2 E[\exp(\beta E)+1]/[\exp(\beta E)-1]. \tag{55}$$

B. Response function in the HO region

In the HO region, the Hamiltonian (22) can be expressed in the HO basis as

$$H = \sum_{\alpha=0}^{1} \epsilon_\alpha a_\alpha^\dagger a_\alpha + E c^\dagger c + \sum_q \hbar\omega_q n_q + \sqrt{W/E}(c^\dagger + c) \sum_{\alpha=0}^{1} g_\alpha a_\alpha^\dagger a_\alpha + i\sqrt{W/E}(c^\dagger + c) \times \sum_q \sqrt{\hbar\omega_q/2\rho\nu_\sigma^2}\,\Lambda_\sigma (b_q - b_q^\dagger), \tag{56}$$

where the bosonic operator c ($c^\dagger$) stands for the annihilation (creation) of a HO. The HO spacing E is given by expression (10). We can make the following identifications:

$$H^{(S)} = \sum_{\alpha=0}^{1} \epsilon_\alpha a_\alpha^\dagger a_\alpha + E c^\dagger c + \sqrt{W/E}(c^\dagger + c) \sum_{\alpha=0}^{1} g_\alpha a_\alpha^\dagger a_\alpha, \tag{57}$$

$$H^{(B)} = \sum_q \hbar\omega_q n_q, \tag{58}$$

$$V^{(S)} = \sqrt{W/E}(c^\dagger + c), \tag{59}$$

$$V^{(B)} = i \sum_q \sqrt{\hbar\omega_q/2\rho\nu_\sigma^2}\,\Lambda_\sigma (b_q - b_q^\dagger). \tag{60}$$

The OAS Hamiltonian can be diagonalized in an exact way. The eigenvalues of this subsystem are given by

$$E_n^\alpha = \epsilon_\alpha + En - g_\alpha^2 W/E^2, \tag{61}$$

and the eigenstates by

$$\Psi_n^\alpha = |\alpha,n\rangle = \chi_n^{\rm HO}(x+Z_\alpha)|\alpha\rangle, \quad \alpha = 0,1; \quad n = 0,\ldots,\infty, \tag{62}$$

with $Z_\alpha = 2g_\alpha W/E^2$. These eigenstates trivially verify the relation

$$\sum_{\alpha,n} |\alpha,n\rangle\langle\alpha,n| = 1. \tag{63}$$

The α index refers to the impurity state and the n index to the HO state or, in terms of excitations, to the number of optical and HO excitations, respectively. The functions $\chi_n^{\rm HO}(x)$ are those of a harmonic oscillator. In this basis we have

$$H^{(S)} = \sum_{\alpha=0}^{1} \sum_{n=0}^{\infty} E_n^\alpha |\alpha,n\rangle\langle\alpha,n|, \tag{64}$$

$$V^{(S)} = \sqrt{W/E}(c^+ + c) - \sum_n \sum_{\alpha=0}^{1} Z_\alpha |\alpha,n\rangle\langle\alpha,n|. \tag{65}$$

Making use of Eqs. (60), (64), and (65), and following the same approximations as in the TLS region, we arrive at

$$F^{\rm HO}(\omega,E) \cong \frac{1}{\pi} |\mu_{10}^{\rm ion}|^2 \rho_{00}^{\rm ion} \sum_{p=-n}^{\infty} \sum_{n=0}^{\infty} \frac{(S^{\rm HO}_{n,p})^2 \rho^{\rm HO}_{n,n} \Gamma^{\rm HO}_{1p,0n}}{[\hbar\omega - \hbar\omega_0 - Ep + (g_1^2 - g_0^2)W/E^2 - \delta^{\rm HO}_{1p,0n}]^2 + (\Gamma^{\rm HO}_{1p,0n})^2}. \tag{66}$$

In this expression, $\rho_{00}^{\rm ion} = \{1+\exp[-\beta\hbar\omega_0 + \beta(g_1^2 - g_0^2)W/E^2]\}^{-1} \cong 1$ is the impurity density matrix diagonal element in its ground state. $\rho^{\rm HO}_{n,n} = [1-\exp(-\beta E)]\exp(-n\beta E)$ is the HO density matrix diagonal element in state n. The elements $S^{\rm HO}_{n,p}$ are the overlap integrals of the HO wave functions between state n with the impurity in its ground state and state $n+p$ with the impurity in its excited state. So, p stands for the number of HO excitations created (or destroyed if $p<0$) in the transition. These elements are given by

$$(S^{\mathrm{HO}}_{n,p})^2=|\langle\chi^{\mathrm{HO}}_{n+p}(x+Z_1)|\chi^{\mathrm{HO}}_{n}(x+Z_0)\rangle|^2=[n!/(n+p)!]^{\mathrm{sgn}(p)}u^{|p|}\ \exp(-u)\mathcal{L}^{|p|}_n(u), \tag{67}$$

with $u\equiv(g_1-g_0)^2W/E^3$ and $\mathcal{L}^n_m(x)$ the associated Laguerre polynomials. As pointed out in the previous section, $\delta^{\mathrm{HO}}_{1p,0n}(E)$ is the shift of the transition that begins at level $(0, n)$, in which the impurity is excited and p HO excitations are created, reaching the level $(1, n+p)$. $\Gamma^{\mathrm{HO}}_{1p,0n}(E)$ is the half-width of that transition. The expressions for both magnitudes are

$$\delta^{\mathrm{HO}}_{1p,0n}(E)=\delta^{\mathrm{HO}}_0(E)\left\{-\frac{8}{3}\frac{W^4(g_1^2-g_0^2)}{E^3}-2W^3\left[\left(2/3+2(E/k_B\Theta_D)^2+(E/k_B\Theta_D)^3\ \ln\left|\frac{1-E/k_B\Theta_D}{1+E/k_B\Theta_D}\right|\right)p\right]\right\}, \tag{68}$$

where

$$\delta^{\mathrm{HO}}_0(E)=[(E/k_B\Theta_D)^3/8\pi^2\rho\hbar^3W^2E]\sum_\sigma\ \Lambda^2_\sigma/\nu^5_\sigma,$$

$$\Gamma^{\mathrm{HO}}_{1p,0n}(E)=\Gamma^{\mathrm{HO}}_0(E)[\coth(\beta E/2)(2n+p)+2n_B(E)], \tag{69}$$

where $\Gamma^{\mathrm{HO}}_0=(WE^2/4\pi\rho\hbar^3)\Sigma_\sigma\Lambda^2_\sigma/\nu^5_\sigma$.

Expression (66) allows us to interpret the line shape of the system under a resonant monochromatic excitation in a simple way: it is formed by an infinite number of Lorentzian lines corresponding to the infinite possible transitions between manifolds $(0, n)$ and $(1, n+p)$, each of them centered at an energy given by $Ep-W(g_1^2-g_0^2)/E^2+\delta^{\mathrm{HO}}_{1p,0n}(E)$ from the impurity resonant transition energy. Each of these Lorentzian lines has a half-width given by $\Gamma^{\mathrm{HO}}_{1p,0n}(E)$ and its intensity is weighed by a thermal factor, the density matrix elements, and an overlap factor, the $S^{\mathrm{HO}}_{n,p}$ elements.

As the impurity-HO coupling is purely nondiagonal, the expression for the response function is valid in the whole range of coupling constant values where Hamiltonian (56) is valid, and we need not distinguish between slow and fast modulation, so the cutoff of the spatial integration will not depend on the HO spacing E. This will have important consequences, as will be shown below.

In general, it is a difficult task to extract any information from expression (66), and one has to resort to numerical evaluations. However, in the weak coupling limit, an analytical expression for $F^{\mathrm{HO}}(\omega)$ can be given, and as will be shown below, this limit is enough to explain the experimental data. So, taking the limit $g_\alpha\ll E$, the only processes that contribute to the HLW are those without creation (or destruction) of HO excitations, i.e., $p=0$, and expression (66) reduces to

$$F^{\mathrm{HO}}(\omega,E)\cong\frac{1}{\pi}\,|\mu^{\mathrm{ion}}_{10}|^2\sum_{n=0}^{\infty}\ \frac{\rho^{\mathrm{HO}}_{n,n}\Gamma^{\mathrm{HO}}_{10,0n}}{(\hbar\omega-\hbar\omega_0)^2+(\Gamma^{\mathrm{HO}}_{10,0n})^2}. \tag{70}$$

The sum in this last expression can be evaluated in terms of hypergeometric functions. However, the resulting expression has not been quoted, as it gives little physical insight into our problem.

As stated above, to obtain the total response of the amorphous solid, we have to average expression (66), or expression (70) in the weak coupling limit, with the density of states (20) and extract the HLW. So, the total response function will be given by

$$\mathcal{F}^{\mathrm{HO}}(\omega)=\int_0^{E_b}dE\ n^{\mathrm{HO}}(E)\int_{V_c}d^3r\ F^{\mathrm{HO}}(\omega,E), \tag{71}$$

where the average over the couplings also has been included. The meaning of the cutoff volume V_c will be discussed in the next section.

It is evident that numerical evaluation of the response function of the whole amorphous solid in the TLS region [expression (54)], or in the HO region [expression (71)], is a very difficult task. We are not presenting it here, as it is planned to be the subject of a future paper.

VI. ANALYTICAL APPROXIMATIONS TO THE HLW

As stated by some authors,[18] the total HLW of the amorphous solid should be extracted from the averaged response function. However, in most cases (see, for example, Refs. 15, 19, 17, and 20), the total HLW is obtained by averaging over the proper HLW for a specific TLS. In Ref. 17 it is argued that this procedure is valid as a series expansion of the total HLW extracted from the total line shape. At this stage, and due to the complexity of the calculations, it is difficult to say whether both procedures (averaging over the response function and averaging over the HLW) would yield similar results. And though we are not trying to answer this question, in this work we shall at least present the results obtained from our model following this approximated method. With this aim, the total HLW averaged over the HLW for a specific soft mode will be calculated in this section.

As stated in the previous section, the half-width of a transition for a specific soft mode of spacing E (TLS or HO) is given by the sum of the half-widths of the levels involved in the transition, weighed by a thermal factor and an overlap factor. So, the HLW of an impurity coupled to a specific soft mode would be given by

$$\Delta\Gamma_H(E,T)=\sum_p\ \sum_n\ \rho^{(S)}_{0n,0n}|\langle 1,n+p|0,n\rangle|^2\Gamma_{1p,0n}, \tag{72}$$

where the particular form of each of the factors in Eq. (72), in terms of the SPM parameters, depends on which region we are dealing with: TLS or HO. The total HLW of the amorphous solid will be given by the average of expression (72) with the adequate density of states. Let us calculate the explicit form of the total HLW in the TLS and HO regions.

A. TLS region

Let us consider expression (72) in the TLS region. We have

$$\Delta\Gamma^{\mathrm{TLS}}_H(E,\Delta_0,T)=2\sum_{n=-1}^{1}\ \sum_{m=-1}^{1}\ \rho^{(S)}_{0m,0m}(S^{\mathrm{TLS}}_{n,m})^2\Gamma^{\mathrm{TLS}}_{1n,0m}, \tag{73}$$

where the particular form of each term has been calculated in Sec. V A.

At this point, we shall take the weak coupling limit, which, as we shall see below, allows one to explain the experimental data. Under this approximation, the factors in Eq. (72) are given by expressions (48), (52), and (53), respectively. So, expression (72) can be put as

$$\Delta\Gamma_H^{\mathrm{TLS}}(E,\Delta_0,T)\cong 8\Gamma_0^{\mathrm{TLS}}\Delta_0^2 E\ \exp(\beta E)/[\exp(\beta E)+1] \times[\exp(\beta E)-1]. \tag{74}$$

The total HLW will be given by the average of the previous expression. Also, the slow modulation limit has to be imposed. So, for a dipole-dipole interaction we have

$$\Delta\Gamma_H^{\mathrm{TLS}}(T)=4\pi\int dE\ d\eta\int_0^{r_0} dr\ r^2 P(E,\eta)\Delta\Gamma_H^{\mathrm{TLS}}(E,\eta,T), \tag{75}$$

where $P(E,\eta)$ is given by Eq. (14) and the spatial integration cutoff by Eq. (55). The integration in the radial coordinate is trivial, leading to

$$\Delta\Gamma_H^{\mathrm{TLS}}(T)=\frac{32\sqrt{2}\pi}{3}\frac{P_s}{W}\,b\int_0^{E_{\max}} dE \times\int_{\tilde{\eta}_0}^{\tilde{\eta}_{\min}}\frac{d\tilde{\eta}}{\sqrt{\tilde{\eta}}}\frac{E}{\sqrt{E^2-\Delta_0^2}}\frac{\exp(\beta E)}{[\exp(\beta E)+1]^2}. \tag{76}$$

In order to evaluate expression (76) numerically, we shall make the usual approximation of neglecting the variations of $\tilde{\eta}_{\min}$ with E. This assumption greatly simplifies the fit to experimental data, as for long time scale experiments this ''effective'' cutoff can be estimated by using the approach described in Ref. 25 of taking the maximum barrier height of the TLS as one-half of the glass transition energy $k_B T_g$, or else it can be taken as a fit parameter in the opposite case. The results obtained from this numerical evaluation are presented in Fig. 3. There, we can see the strong dependence of the HLW on this cutoff in the TLS region: it ranges from a linear law for large values of $\tilde{\eta}_{\min}$ (long experimental time scale) to a non-power-law for small values of $\tilde{\eta}_{\min}$ (short experimental time scale). Also, the magnitude is slightly dependent on this cutoff. As quoted in Fig. 3, for some values of $\tilde{\eta}_{\min}$, a $T^{1.3}$ dependence is obtained below W/k_B, which seems to indicate there is no need to introduce any parameters for the density of states of TLS as was suggested by some authors.[32] Above $E_{\max}/k_B$ the HLW behaves closely as a constant. These results are only slightly modified if we leave aside the above approximation.

Nevertheless, in the limit of diagonal modulation introduced above, an analytical expression for the total HLW in the TLS region can be obtained. In this case, we can average by making use of the density of states (15), and in this way obtain an expression for the total HLW below $E_{\max}/k_B$:

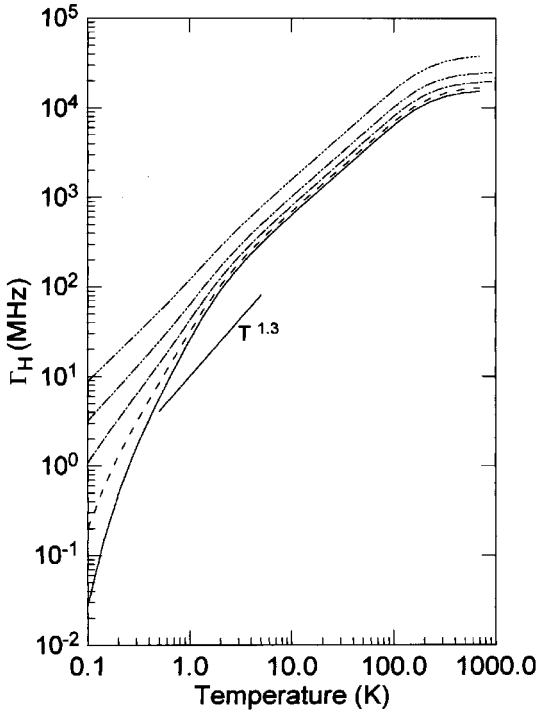

FIG. 3. HLW in the TLS region for some $\tilde{\eta}_{\min}$ values. (—): $\tilde{\eta}_{\min}=2.87$; (- - -): $\tilde{\eta}_{\min}=3.43$; (–·–·–): $\tilde{\eta}_{\min}=4.57$; (–···–): $\tilde{\eta}_{\min}=7.25$; (–···–): $\tilde{\eta}_{\min}=17.5$.

$$\Delta\Gamma_H^{\mathrm{TLS}}(T)=\frac{8\pi}{3}\,n^{\mathrm{TLS}} b k_B T, \tag{77}$$

with n^{TLS} given by Eq. (18), which coincides with the one calculated by Lyo[15] in the same limit, but starting from the tunneling states model.

B. HO Region

Let us consider expression (72) for a specific HO. We have

$$\Delta\Gamma_H^{\mathrm{HO}}(E,T)=\sum_{p=-n}^{\infty}\sum_{n=0}^{\infty}\rho_{00}^{\mathrm{ion}}\rho_{n,n}^{\mathrm{HO}}|\langle\chi_{p+n}^{\mathrm{HO}}(x+Z_1) \times|\chi_n^{\mathrm{HO}}(x+Z_0)\rangle|^2\Gamma_{1p,0n}^{\mathrm{HO}}. \tag{78}$$

It is convenient to separate transitions with HO creation ($p>0$) from transitions with HO annihilation ($p<0$). So, we make

$$\Delta\Gamma_H^{\mathrm{HO}}(E,T)=\Delta\Gamma_H^{\mathrm{HO}}(E,T)^{p\geqslant 0}+\Delta\Gamma_H^{\mathrm{HO}}(E,T)^{p<0}, \tag{79}$$

where

$$\Delta\Gamma_H^{\mathrm{HO}}(E,T)^{p\geqslant 0}=\Gamma_0^{\mathrm{HO}}\exp(-u)\sum_{p=0}^{\infty}\sum_{n=0}^{\infty}\frac{n!}{(n+p)!}t^n u^p\mathcal{L}_n^p(u)^2[(1+t)(2n+p)+2t], \tag{80}$$

$$\Delta\Gamma_H^{\mathrm{HO}}(E,T)^{p<0}=\Gamma_0^{\mathrm{HO}}\exp(-u)\sum_{p=0}^{\infty}t^p\sum_{n=0}^{\infty}\frac{n!}{(n+p)!}t^n u^p\mathcal{L}_n^p(u)^2[(1+t)(2n+p)+2t], \tag{81}$$

with $t=\exp(-\beta E)$. Taking into account the relations

$$\sum_{n=0}^{\infty} \frac{n!}{(n+p)!}\, t^n \mathcal{L}_n^p(u)^2 = \frac{u^{-p} t^{-p/2}}{1-t} \exp\left(-\frac{2ut}{1-t}\right) I_p\left(\frac{2ut^{1/2}}{1-t}\right), \tag{82}$$

$$\sum_{n=0}^{\infty} \frac{n!}{(n+p)!}\, (n+1) t^n \mathcal{L}_n^p(u)^2 = \sum_{n=0}^{\infty} \frac{n!}{(n+p)!} \frac{\partial}{\partial t^n}\, t^{n+1} \mathcal{L}_n^p(u)^2, \tag{83}$$

$$\frac{\partial}{\partial z} I_p(z) = \frac{1}{2}\left[I_{p-1}(z) + I_{p+1}(z)\right], \tag{84}$$

where $I_p(z)$ is the Bessel function of the first kind with an imaginary argument, we arrive at

$$\Delta\Gamma_H^{\mathrm{HO}}(E,T) = \Gamma_0^{\mathrm{HO}}\left[\mathrm{csch}^2(\beta E/2) + u\ \coth(\beta E/2)\right]. \tag{85}$$

The total HLW will be given by the average of this expression with the density of states (20):

$$\Delta\Gamma_H^{\mathrm{HO}}(T) = \langle \Delta\Gamma_H^{\mathrm{HO}}(E,T)\rangle_{E,r} = \frac{P_s}{3\sqrt{2}\pi\rho W^4 \hbar^3}\, V_c \sum_{\sigma} \frac{\Lambda_\sigma^2}{\nu_\sigma^5} (k_B T)^7 \int_0^{E_b/k_B T} dx\, \frac{x^6 e^x}{(e^x-1)^2}, \tag{86}$$

in the weak-impurity–HO coupling limit. The volume in which the HO is localized,[10] V_c, appears when we properly normalize the distribution function to the total number of soft modes in the solid. In fact, the integration over the spatial coordinate r extends along the whole volume of the amorphous solid, V. As the total number of soft modes is finite and equal to N, we must divide by this normalization constant, thus obtaining a factor $V/N_{\mathrm{HO}} = V_c$, which is nothing but the volume where the soft mode is localized. This macroscopic parameter can be related to another parameter, which can be estimated from neutron scattering data: the number of atoms and/or molecules participating in the mode N_s,[10] through the relation $V_c = N_s M_{\mathrm{molecular}}/\rho$, where $M_{\mathrm{molecular}}$ is the mole mass in grams of the atoms and/or molecules conforming the mode.

Expression (86) is valid for a general form of the impurity-HO interaction, as long as $\Delta\Gamma_H^{\mathrm{HO}}(E,T)$ contains a (g_1-g_0)-independent term and the coupled impurity-HO system can be treated as a coherent state, i.e., when the coupling is sufficiently strong. This can be expressed in an analytical way by the condition $b/r^s \gg \Gamma$ for a multipolar coupling, where Γ is the characteristic broadening of the HO and is given by $\Gamma \sim \Gamma_0^{\mathrm{HO}}$. In other words, our treatment is valid only for those HO with a characteristic decay rate in the continuum of phonons that is slow enough to form a coherent impurity-HO state, i.e., $r \ll (b/\Gamma)^s$. Obviously, the case in which the approximation works worst is for $E = E_b$. If we now define r_{cohe} as the smallest value of r where the previous inequality holds, and consider a dipole-dipole interaction $(s=3)$, with b values given by those calculated in the TLS region, we obtain $r_{\mathrm{cohe}} \cong 8$ Å for the SiO_2 and $r_{\mathrm{cohe}} \cong 26$ Å for the PMMA (polymethyl methacrylate), while $r_0 = (3V_c/4\pi)^{1/3}$ is 5 Å and 10 Å for the SiO_2 and PMMA cases, respectively, so the coherence limit is fulfilled (see Table I and the Sec. VII for details about the calculation of the various parameters). In the case of a dipole-quadrupole interaction it is difficult to establish a comparison between r_{cohe} and r_0, as we have no reliable estimations of the coupling b.

For temperatures much lower than E_b we can evaluate Eq. (86) to give

$$\Delta\Gamma_H^{\mathrm{HO}} \cong \frac{16\pi^5 P_s}{63\sqrt{2}\rho W^4 \hbar^3}\, V_c \sum_{\sigma} \frac{\Lambda_\sigma^2}{\nu_\sigma^5} (k_B T)^7, \tag{87}$$

and for temperatures above E_b we have

$$\Delta\Gamma_H^{\mathrm{HO}} \cong \frac{P_s E_b^5}{15\sqrt{2}\pi\rho W^4 \hbar^3}\, V_c \sum_{\sigma} \frac{\Lambda_\sigma^2}{\nu_\sigma^5} (k_B T)^2. \tag{88}$$

So, this mechanism has the same behavior as Raman processes in crystalline materials, but the high- and low-temperature limits are defined in terms of E_b, which is characteristic of the amorphous solids and is usually one order of magnitude lower than the Debye temperature.

VII. RESULTS OF THE NUMERICAL EVALUATION OF THE HLW

Expressions (76) and (86) have been evaluated numerically for some materials and the results are presented in Fig. 4. These materials have been chosen in an attempt to give a complete picture throughout a broad temperature range. The various parameters of the SPM have been quoted in Table I for each material. They have been calculated from TS model parameter measurements in the low-temperature regime, following the procedure in Ref. 25. Unfortunately, the coupling b and the volume V_c (or, equivalently, the participating number N_s) are not known in general, and only estimations for vitreous silica and a few other materials were available.[10] So, we have taken them as fitting parameters. The deduced values also have been quoted in Table I. An exception is the system Nd^{3+}:SiO_2, where all the SPM parameters are well known, and a reliable estimation of N_s exists.[10] Unfortunately, there are no experimental data for this system in the medium to high temperature range.

Let us try to analyze Fig. 4. The first striking feature is the excellent agreement between experimental data and numeri-

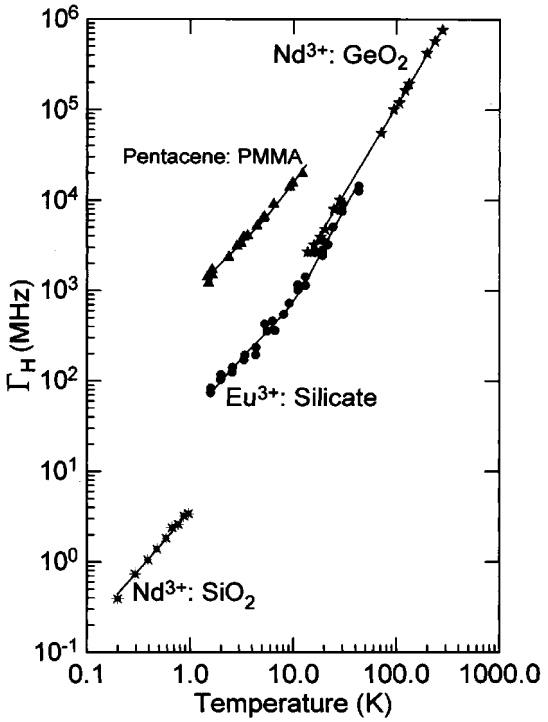

FIG. 4. Numerical (solid lines) and experimental data of the HLW for some systems: (▲) Pentacene: PMMA (Ref. 33) (★): Nd^{3+}: GeO_2 (Ref. 32); (●): Eu^{3+}: Silicate (Ref. 34) (*): Nd^{3+}: SiO_2 (Ref. 35). Numerical data have been evaluated by making use of expressions (76) and (86) in the TLS and HO regions, respectively.

cal fits in the whole temperature range and for all the materials studied. The Eu^{3+}: silicate system is worth mentioning, as this is one of the few systems in which a crossover from a linear to a quadratic law has been clearly observed. We can see that the combination of the two mechanisms proposed here accurately describes this crossover. The pentacene: PMMA data are also well described by our model, and, in contrast to the usually accepted $T^{1.3}$ law, we find a better agreement when considering a combination of both mechanisms; however, it is reasonable to expect such a supralinear behavior for lower temperatures, as this kind of crossover appears below W/k_B as shown by Eq. (76). For the Nd^{3+}:SiO_2 system, and choosing a reasonable value for the cutoff $\tilde{\eta}_{\min}$ (this value, and the ones estimated for the other systems using the method described in Sec. VI A, have been quoted in Table I), we are able to describe the $T^{1.3}$ power law exhibited by the experimental data. In the measured region, the HO contribution can be neglected. The Nd^{3+}:SiO_2 and Nd^{3+}:GeO_2 systems are expected to exhibit a very similar behavior, as the host matrices' structures are very alike; however, the experimental data of Nd^{3+}:GeO_2, if extrapolated to low temperatures, are one order of magnitude larger than those of Nd^{3+}:SiO_2. This is a surprising fact, which will be discussed below. Anyway, the Nd^{3+}:GeO_2 data are also well fitted, though it is worth saying we have to combine both mechanisms to describe the whole set of data, which seems to indicate a moderate crossover below 10 K.

Let us now discuss the calculated fitting parameters b and N_s. For reasons suggested above, we can expect the number of participating molecules in GeO_2 to be very similar to the one in SiO_2. The better fit to experimental data gives a value of almost 12 molecules participating in the soft mode, in complete agreement with the estimation made by Buchenau *et al.* in Ref. 10 for SiO_2. Although we have no reliable estimations of the number of participating molecules in silicate and PMMA glasses, the same reference points to participating numbers between 20 and 100 atoms and/or molecules per soft mode, the same as the ones we have obtained. The values of parameter b are also in good agreement with usually accepted values (see Ref. 35) for an electrostatic dipole-dipole interaction. Let us now return to a puzzling question. As mentioned above, Nd^{3+}:GeO_2 experimental data are one order of magnitude larger than Nd^{3+}:SiO_2 ones, which leads to a difference of one order of magnitude in the corresponding b couplings. These two facts have no easy explanation if, as we have admitted, both systems have an almost identical microscopic structure. In fact, this behavior has been already pointed out by some authors[32] in other systems, and it has been related to the different experimental techniques that have characteristic measurement and detection times lying in different time scales, which in turn fix the cutoff $\tilde{\eta}_{\min}$, on which the density of TLS depends. Though it is out of the scope of our work, we think this question deserves a deeper study. Concerning this point, we would like to add some additional comments about this time dependence of the HLW. As can be seen from expressions (15) and (18), we can expect a time dependence of the TLS density of states even in the most simple limit, which should reflect on every measurable physical quantity such as, for example, the HLW. This time dependence has been experimentally observed, but its nature is not yet clearly understood, and is usually ascribed to some kind of spectral diffusion mechanism. As can be seen in expression (76), this time dependence also appears in our model if the variation of $\tilde{\eta}_{\min}$ with time is taken into account. More work in this direction should be desirable, and is planned to be the subject of a future paper.

VIII. CONCLUSIONS

We can conclude that our model gives a very accurate description of the experimental data in any temperature range, without introducing any adjustable exponents for the TLS density of states. Moreover, a very interesting feature of this model is to establish relations between optical dephasing properties and other kinds of properties, through energy E_b, which defines the low- and high-temperature limits of the HO contribution. We think more attention should be paid to the question of relating optical dephasing properties to thermal and transport ones.

A striking point that is worthy of attention is the independence of the HO contribution on the coupling. This means that for the same host, HLW would be almost independent of impurity in the high-temperature limit. It should be desirable to have experimental confirmation of this fact. In any case, let us remember we have neglected a coupling-dependent term in expression (85), which is expected to vary with each impurity. This part contains a temperature-independent contribution that would dominate the HLW at ultralow temperatures in some coupling ranges, and could be related to those temperature-independent contributions of various GHz ob-

served in some organic systems.[32]

Finally, we wish to emphasize that the problem of impurity HLW in glasses is far from being completely solved. We think that more experimental work in some simple systems is desirable to contrast different theoretical models. Also, the question of the HLW dependence with time requires more theoretical studies. Moreover, numerical studies in the crossover region between TLS and HO would be also necessary.

ACKNOWLEDGMENT

This work was supported by the Spanish Government CICYT (Ref. MAT. 0434/93)

APPENDIX A: THE SOFT-MODE PARAMETER DISTRIBUTION FUNCTION

In this Appendix we deduce the distribution function (11) on the basis of the Ramos *et al.*[25] work. The soft potential can be written in two equivalent forms:

$$V(x)=W[\eta(x/a)^2+\xi(x/a)^3+(x/a)^4] \tag{A1}$$

or

$$V(x)=W[D_1(x/a)+D_2(x/a)^2+(x/a)^4]. \tag{A2}$$

The relation between both sets of parameters is given by

$$D_1=-\eta\xi/2+\xi^3/8, \tag{A3}$$

$$D_2=\eta-3\xi^2/8. \tag{A4}$$

The probability distribution $P(\eta,\xi)$ of the random parameters η and ξ as a function of η is assumed to be centered near $\eta\sim 1$, which corresponds to the standard atomic potentials. The soft potentials then occur in the region of the tail of the distribution $P(\eta,\xi)$, within the range of low values of η. It can be shown that in the limit $|\eta|\ll 1$, $P(\eta,\xi)$ is finite and takes the form[22]

$$P(\eta,\xi)=|\eta|\mathcal{P}_0(\eta,\xi), \tag{A5}$$

where $\mathcal{P}_0(\eta,\xi)$ is a smooth function. $\mathcal{P}_0(\eta,\xi)$ as a function of ξ is assumed to be even, due to the absence of a preferred direction in a glass. Referring to variables (D_1,D_2), it can be seen that the easiest way to characterize the distribution of the random parameters η and ξ (with the exception of the constant function), with the previous conditions being fulfilled, is by means of the function[25]

$$P(D_1,D_2)=P_s\ \exp(-AD_1^2), \tag{A6}$$

where the scale for the coefficient of D_1^2, A, is estimated by assuming that the asymmetry D_1 is due to thermal strains, which freeze in at the glass transition temperature T_g so this scale is given by $A=0.169(W/k_BT_g)^{3/2}$. By making use of Eqs. (A3), (A4), and (A6) we arrive at expression (11) for the distribution function in the (η,ξ) variables.

APPENDIX B: RESPONSE FUNCTION IN THE FRAMEWORK OF THE ZWANZIG-FANO RELAXATION THEORY

Let us consider a system with known energy levels and that is able to couple to an electromagnetic field. Let us assume that the system is interacting with a thermal bath. The Hamiltonian of the whole system+bath set is given by

$$H=H^{(S)}+H^{(B)}+H_{\rm int}, \tag{B1}$$

where $H^{(S)}$ refers to the optically active subsystem, $H^{(B)}$ to the bath, and $H_{\rm int}$ refers to the interaction between both systems. For many cases of interest, the interaction between the optically active subsystem (OAS) and the thermal bath can be factorized as

$$H_{\rm int}=V^{(S)}\cdot V^{(B)}, \tag{B2}$$

where $V^{(S)}$ refers to the OAS, and $V^{(B)}$ to the bath. We will assume that the eigenvectors of $H^{(S)}$, denoted by $|i\rangle,|f\rangle,\ldots$, form a discrete set, whereas those of $H^{(B)}$, denoted by $|\alpha\rangle,|\beta\rangle,\ldots$, are dense and form a quasicontinuum.

Following the Zwanzig-Fano relaxation theory,[31] the response of the OAS under an electromagnetic external perturbation can be calculated to any order in the interaction. The technique essentially consists in eliminating the thermal bath variables from the physical quantities of interest by the introduction of an adequate projection operator over the OAS Hilbert subspace. Using this method, we are able to calculate the line shape of the OAS optical transitions in contact with a phonon thermal bath. The expression for this function, to which we arrive in the framework of this theory, is given by

$$F(\omega)=-\frac{1}{\pi}\,\mathrm{Im}\sum_{f,i}|\mu_{fi}^{(S)}|^2\rho_{ii}^{(S)}\times\frac{1}{\hbar\omega-\hbar\omega_{fi}-\langle M_c(\hbar\omega+i\eta^+)\rangle_{fi,fi}}. \tag{B3}$$

The notation used is as follows: $\mu_{fi}^{(S)}$ denotes OAS dipole moment operator element between the states f and i. $\rho_{ii}^{(S)}$ denotes OAS density matrix diagonal element. $\hbar\omega_{fi}=E_{fi}$ denotes OAS transition energy between f and i states. $\langle M_c(\hbar\omega+i\eta^+)\rangle_{fi,fi}$ denotes element of the so-called memory function of the system between the states (fi) and (fi), properly averaged over the bath variables. This is a linear operator over the linear operators space of the OAS Hilbert space, so it has four indexes. This function allows for an iterative equation:

$$M_c(z)=L_1+L_1\frac{1}{z-L_0}(1-P)M_c(z), \tag{B4}$$

where L_0 is the Liouville operator of the free part of the Hamiltonian, operationally defined as

$$L_0=[H^{(S)}+H^{(B)},\ ], \tag{B5}$$

L_1 is the Liouville operator of the interaction, given by

$$L_1=[H_{\rm int},\ ], \tag{B6}$$

where [,] is the conmutator. Finally, $P=|\rho^{(B)}\rangle\rangle\langle\langle \mathbf{1}^{(B)}|$ is a projector over the OAS Hilbert subspace, with $\rho^{(B)}$ the thermal bath density matrix and $\mathbf{1}^{(B)}$ the identity operator over the bath Hilbert subspace. The double ket indicates that these operators are vectors of the linear operators space over the Hilbert space. The memory function contains all the dynamical effects of the OAS-bath interaction.

Using Eq. (B4), it is straightforward to obtain a perturbative expression of the memory function operator to a second order in the interaction:[31]

$$\langle M_c(z)\rangle_{fi,fi}=\Delta V+K(z), \tag{B7}$$

where

$$\Delta V=(V_{ff}^{(S)}-V_{ii}^{(S)})\langle V^{(B)}\rangle, \tag{B8}$$

$$K(z)=\sum_{\alpha,\beta} w_\beta(|\langle\alpha|V^{(B)}|\beta\rangle|^2-\langle V^{(B)}\rangle^2\delta_{\alpha\beta})\left[\sum_k\left(\frac{|V_{fk}^{(S)}|^2}{z-E_{ki}-E_{\alpha\beta}}+\frac{|V_{ik}^{(S)}|^2}{z-E_{fk}-E_{\beta\alpha}}\right)-V_{ff}^{(S)}V_{ii}^{(S)}\left(\frac{1}{z-E_{fi}-E_{\beta\alpha}}+\frac{1}{z-E_{fi}+E_{\beta\alpha}}\right)\right]. \tag{B9}$$

The following notation has been used in expressions (B8) and (B9):

$$V_{kl}^{(S)}=\langle k|V^{(S)}|l\rangle, \tag{B10}$$

$$V^{(B)}=\sum_\beta w_\beta\langle\beta|V^{(B)}|\beta\rangle, \tag{B11}$$

where $w_\beta=\exp(-E_\alpha/k_BT)/\Sigma_{\alpha'}\exp(-E_{\alpha'}/k_BT)$ are the density matrix operator diagonal elements of the thermal bath, provided this is a canonical distribution over the bath variables and, so, diagonal in the eigenstates of $H^{(B)}$.

The memory function will be a complex number in the general case, so we can separate the imaginary and real parts:

$$\delta_{fi}=\mathrm{Re}[\langle M_c(\hbar\omega_{fi}+i\eta^+)\rangle_{fi,fi}], \tag{B12}$$

$$\Gamma_{fi}=-\mathrm{Im}[\langle M_c(\hbar\omega_{fi}+i\eta^+)\rangle_{fi,fi}], \tag{B13}$$

where $\hbar\omega_{fi}=E_f-E_i$. Substituting in expression (B3) we arrive at

$$F(\omega)=\frac{1}{\pi}\sum_{f,i}|\mu_{fi}^{(S)}|^2\rho_{ii}^{(S)}\frac{\Gamma_{fi}}{(\hbar\omega-\hbar\omega_{fi}-\delta_{fi})^2+\Gamma_{fi}^2}, \tag{B14}$$

so δ_{fi} represents the shift of the OAS $|f\rangle$ to $|i\rangle$ transition and Γ_{fi} the half-width of this transition.

A more detailed presentation of the technique used and a discussion about the approximations that lead to expression (B3) can be found in Ref. 31 or in the original works by Zwanzig and Fano.[36,37]

APPENDIX C: EVALUATION OF THE MEMORY FUNCTION IN THE TLS AND HO REGIONS

Let us consider expression (B7) of the memory function. As the OAS-bath interaction cannot connect states with the same phonon occupation number, the ΔV term is null, so the memory function is equal to $K(z)$. Let us calculate the elements of the interaction Hamiltonian:

1. TLS region

Expanding the elements $\langle\alpha|V^{(B)}|\beta\rangle$, we arrive at an expression for $\langle M_c(z)\rangle_{fi,fi}$:

$$\langle M_c(z)\rangle_{fi,fi}=\sum_q|D_q|^2[\overline{n_q}F_-(E_q)+(\overline{n_q}+1)F_+(E_q)], \tag{C1}$$

where $\overline{n_q}$ are the mean phonon occupation numbers in mode q, $|D_q|^2=(E_q/2\rho\nu_\sigma^2)\gamma_\sigma^2$ and

$$F_\pm(E_q)=\sum\left(\frac{|V_{fk}^{(S)}|^2}{z-E_{ki}\mp E_q}+\frac{|V_{ik}^{(S)}|^2}{z-E_{jk}\pm E_q}\right)-V_{ff}^{(S)}V_{ii}^{(S)}\times\left(\frac{1}{z-E_{fi}\pm E_q}+\frac{1}{z-E_{fi}\mp E_q}\right). \tag{C2}$$

Taking into account that, for our system, $|k\rangle=|\rho^k,n^k\rangle$, where $\rho^k=0,1$ stands for the impurity state and $|n^k\rangle=\pm1$ stands for the TLS level, and expanding the sums in expression (B3), we arrive at the conclusion that we only need to evaluate the element $\langle M_c(E_{1n^f0n^i}+i\eta^+)\rangle_{1n^f0n^i,1n^f0n^i}$ (in the Markovian approximation). Doing so, and once we expand the $V_{kl}^{(S)}$ elements, we obtain

$$F_\pm(E_q)=\frac{A_1^2}{\mp E_q+i\eta^+}+\frac{A_0^2}{\pm E_q+i\eta^+}+\frac{B_1^2}{n^f\varepsilon_1\mp E_q+i\eta^+}+\frac{B_0^2}{n^i\varepsilon_0\pm E_q+i\eta^+}+A_0A_1\left(\frac{1}{\pm E_q+i\eta^+}+\frac{1}{\mp E_q+i\eta^+}\right). \tag{C3}$$

Making use of the well-known relation

$$\frac{1}{x+iy}=\mathrm{P}\left(\frac{1}{x}\right)-i\pi\delta(x), \tag{C4}$$

with P the principal value, we can separate the imaginary and real parts of the memory function element, and obtain the shift and the half-width of the transition. In doing so, we arrive at

$$\delta_{1n^f0n^i}=\sum_q |D_q|^2\{\overline{n_q}\,\mathrm{Re}[F_-(E_q)]+(\overline{n_q}+1)\mathrm{Re}[F_+(E_q)]\}, \tag{C5}$$

$$\Gamma_{1n^f0n^i}=-\sum_q |D_q|^2\{\overline{n_q}\,\mathrm{Im}[F_-(E_q)] +(\overline{n_q}+1)\mathrm{Im}[F_+(E_q)]\}, \tag{C6}$$

where

$$\mathrm{Re}[F_\pm(E_q)]=\mathrm{P}\left[\frac{A_1^2}{\mp E_q}+\frac{A_0^2}{\pm E_q}+\frac{B_1^2}{n^f\varepsilon_1\mp E_q}+\frac{B_0^2}{n^i\varepsilon_0\pm E_q}\right], \tag{C7}$$

$$\mathrm{Im}[F_\mp(E_q)]=-\pi[B_1^2\delta(n^f\varepsilon_1\mp E_q)+B_0^2\delta(-n^i\varepsilon_1\pm E_q)]. \tag{C8}$$

In the last expression, only the terms that have a nonzero sum have been included. Using the Debye density of states and dispersion relation, we can evaluate the sums in (C5) and (C6), and obtain in this way expressions (42) and (43) of the text.

2. HO region

We just have to follow the same steps of the previous region, which lead to

$$\mathrm{Re}[F_\pm(E_q)]=\mathrm{P}\left\{\frac{W}{E}\left[\frac{n^f}{E+E_q}+\frac{n^f+1}{-E+E_q}-\frac{n^i}{E+E_q}+\frac{n^i+1}{E-E_q}\right] +4\frac{W^2}{E^4}\frac{(g_1^2-g_0^2)}{E_q}\right\}, \tag{C9}$$

$$\mathrm{Im}[F_\pm(E_q)]=-\pi\left[\frac{W}{E}\binom{n^f+n^i+2}{n^f+n^i}\delta(E-E_q)\right], \tag{C10}$$

where the upper (lower) term inside the parentheses refers to the $+$ $(-)$ sign, respectively. In order to recover the notation used throughout the paper, we must change from the pair of quantum numbers (n^i,n^f) to $(n=n^i,p=n^f-n^i)$. In doing so, and once we evaluate the sums over phonon modes in the Debye model, we obtain expressions (68) and (69) of the text.

[1] R. C. Zeller, and R. O. Pohl, Phys. Rev. B **4**, 2029 (1971).
[2] *Amorphous Solids: Low Temperature Properties*, edited by W. A. Phillips (Springer, Berlin, 1981).
[3] P. W. Anderson, B. I. Halperin, and C. M. Varma, Philos. Mag. **25**, 1 (1972).
[4] W. A. Phillips, J. Low Temp. Phys. **7**, 351 (1972).
[5] A. C. Anderson, in *Amorphous Solids: Low Temperature Properties* (Ref. 2).
[6] V. K. Malinovsky *et al.*, Europhys. Lett. **11**, 43 (1990).
[7] U. Buchenau *et al.*, Phys. Rev. Lett. **60**, 1318 (1991).
[8] V. G. Karpov, M. I. Klinger, and F. N. Ignat'ev, Zh. Eksp. Teor. Fiz. **84**, 760 (1983) [Sov. Phys. JETP **57**, 439 (1983)].
[9] U. Buchenau *et al.*, Phys. Rev. B **46**, 2798 (1992).
[10] U. Buchenau *et al.*, Phys. Rev. B **43**, 5039 (1991).
[11] A. Fontana *et al.*, Philos. Mag. B **71**, 525 (1995).
[12] *Optical linewidths in glasses*, edited by Marvin J. Weber, special issue of J. Lumin. **36**, 179 (1987).
[13] B. Henderson and G. F. Imbusch, *Optical Spectroscopy of Inorganic Solids* (Claredon Press, Oxford, 1989).
[14] T. L. Reinecke, Solid State Commun. **32**, 1103 (1979).
[15] S. K. Lyo, Phys. Rev. Lett. **48**, 688 (1982).
[16] S. K. Lyo, in *Optical Spectroscopy of Glasses*, edited by I. Zschokke (D. Reidel, Dordrecht, 1986).
[17] R. Reineker and H. Morawitz, Chem. Phys. Lett. **86**, 359 (1982).
[18] P. Reineker and K. Kassner, in *Optical Spectroscopy of Glasses*, edited by I. Zschokke (D. Reidel, Dordrecht, 1986).
[19] H. Morawitz and P. Reineker, Solid State Commun. **42**, 609 (1982).
[20] P. Reineker, H. Morawitz, and K. Kassner, Phys. Rev. B **29**, 4546 (1984).
[21] S. K. Lyo and R. Orbach, Phys. Rev. B **29**, 2300 (1984).
[22] M. A. Il'in, V. G. Karpov, and D. A. Parshin, Zh. Eksp. Teor. Fiz. **92**, 291 (1987) [Sov. Phys. JETP **65**, 165 (1987)].
[23] The scale η_L appears in the denominator because we have changed the definition of Λ_l and Λ_t as compared to those of Ref. 9 by a factor $\eta_L^{1/2}$.
[24] V. L. Gurevich *et al.*, Phys. Rev. B **48**, 16 318 (1993).
[25] M. A. Ramos, L. Gil, and U. Buchenau, Phys. Status Solidi B **135**, 477 (1993).
[26] L. Gil *et al.*, Phys. Rev. Lett. **70**, 182 (1993).
[27] R. O. Pohl, in *Amorphous Solids: Low Temperature Properties* (Ref. 2).
[28] J. F. Berret and M. Meissner, Z. Phys. B **70**, 65 (1988).
[29] For $A(W/E)^6\ll 1$ we made a series expansion of the integrand and, in the opposite limit, we made a saddle-point approximation.
[30] In these 4×4 matrices, σ_i is the 2×2 ith Pauli matrix and $0_{2\times2}$ is the null 2×2 matrix.
[31] M. J. Burns, W. K. Liu, and A. H. Zewail, in *Spectroscopy and Excitation Dynamics of Condensed Molecular Systems*, edited by V. M. Agranovich and R. M. Hochstrasser (North-Holland, Amsterdam, 1983).
[32] R. M. MacFarlane and R. M. Shelby, in *Optical Linewidths in Glasses* (Ref. 12).
[33] S. Völker, in *Optical Linewidths in Glasses* (Ref. 12).
[34] R. Yano, M. Mitsunaga, N. Uesugi, and M. Shimizu, Phys. Rev. B **50**, 9031 (1994).
[35] D. L. Huber, M. M. Broer, and B. Golding, Phys. Rev. Lett. **52**, 2281 (1984).
[36] R. Zwanzig, J. Chem. Phys. **33**, 1338 (1960).
[37] U. Fano, Phys. Rev. **131**, 259 (1963).